Water Research 105 (2016) 47–55

Contents lists available at ScienceDirect

Water Research

journal homepage: www.elsevier.com/locate/watres

# Bioaccumulation and ecotoxicity increase during indirect photochemical transformation of polycyclic musk tonalide: A modeling study

Yanpeng Gao [a], Yuemeng Ji [b], Guiying Li [b], Bixian Mai [a], Taicheng An [a, b, *]

[a] State Key Laboratory of Organic Geochemistry and Guangdong Key Laboratory of Environmental Resources Utilization and Protection, Guangzhou Institute of Geochemistry, Chinese Academy of Sciences, Guangzhou 510640, China
[b] Institute of Environmental Health and Pollution Control, School of Environmental Science and Engineering, Guangdong University of Technology, Guangzhou 510006, China

ARTICLE INFO

*Article history:*
Received 6 June 2016
Received in revised form
25 August 2016
Accepted 26 August 2016
Available online 28 August 2016

*Keywords:*
Polycyclic musks
Phototransformation process
Hydroxyl radical
Theoretical calculation
Bioaccumulation

ABSTRACT

Polycyclic musks (PCMs) have recently caused a worldwide environmental concern due to their bioaccumulation potential and ecotoxicological effects. Herein, the •OH-initiated indirect photochemical transformation mechanism, environmental fate and ecotoxicity of PCMs (by taking tonalide as an example) were theoretically studied. Results show that tonalide can be degraded readily through •OH-addition and H-abstraction pathways, with total rate constants of $6.03 \times 10^9$–$15.8 \times 10^9$ $M^{-1}$ $s^{-1}$. The •OH-addition pathways were dominant at low temperature (<~287 K), whereas H-abstraction was the dominant pathway at high temperature. Further, the bioconcentration factors (BCF) and aquatic toxicities to fish of all transformation products from H-abstraction pathways were smaller than tonalide. In contrast, these values of most intermediates from •OH-addition pathways were up to 8 times higher than tonalide. Particularly, the resultant phenolic product PC1 had a BCF of 5590 L/kg wet-wt, which exceeds the cutoff criterion set for the typically persistent organic pollutants as critically bioaccumulative. Notably, PC1 would mainly be produced under anaerobic aquatic conditions at low temperatures. Therefore, particular attention should be paid to the indirect photochemical products and parental PCMs, particularly the intermediates from •OH-addition pathway.



## 1. Introduction

Polycyclic musks (PCMs) are not only used as fragrance ingredients in perfumes, cosmetics, detergents and other scented personal care products, but also as additives in cigarettes, and fish baits (Heberer, 2003). Among these PCMs, tonalide along with galaxolide are two of the most frequently used products. Both of them represent approximately 95% of PCMs within the EU market (Clara et al., 2011). Given the extensive use and high consumption, tonalide and other PCMs are continuously discharged into aquatic environment. Their concentrations are quite variable depending on the proximity of urban or rural center and their corresponding discharge points. In addition, the removal efficiencies of conventional wastewater treatment plants (WWTP) were reported as 25.5%–70.1% for PCMs (Zhou et al., 2009). As a result, they appear at ng/L concentrations in WWTP effluent and receiving bodies (Chase et al., 2012). Especially, tonalide and galaxolide at the highest levels were the predominant PCMs (Lu et al., 2015). These PCMs would not only contaminate the water environment, but also were frequently found in aquatic organisms as well as accumulate in aquatic organisms (Chen et al., 2015; Fernandes et al., 2013; Fromme et al., 2001a; Kannan et al., 2005; Luckenbach and Epel, 2005), and even human milk, blood, and adipose tissues (Schiavone et al., 2010). More important, when released into water, PCMs may transform into other products. Also, it is worth noting that the levels of several transformation products in water were higher than their parental PCMs (Gómez et al., 2012; Lange et al., 2015). As such, the aquatic ecosystems are exposed to an unknown cocktail of PCMs and transformation products. Therefore, it is of great concern to unmask the transformation mechanisms, kinetics, and fate of PCMs in aquatic environments. Further, the

* Corresponding author. Institute of Environmental Health and Pollution Control, School of Environmental Science and Engineering, Guangdong University of Technology, Guangzhou, 510006, China.
*E-mail address:* antc99@gdut.edu.cn (T. An).

http://dx.doi.org/10.1016/j.watres.2016.08.055
0043-1354/

exposure risk of PCMs and their transformation products to aquatic organisms also needs to be investigated.

Photochemical pathway is generally considered as an important potential transformation process for PCMs in water, because their biodegradation and hydrolysis are slow (Buerge et al., 2003; Lucía Sanchez-Prado et al., 2004). Previous experiments showed that both tonalide and galaxolide are quite photochemically unstable (Buerge et al., 2003; Santiago-Morales et al., 2012), and the photodegradation rate of tonalide was approximately 12–30 times quicker than galaxolide under UV irradiation in laboratory (Buerge et al., 2003; Lucía Sanchez-Prado et al., 2004). This suggests that tonalide is more easily photo-transformed than galaxolide. However, the photochemical transformation of PCMs is mainly focused on galaxolide. As for tonalide, the photochemical transformation mechanisms and environmental impacts in natural waters are rarely discussed. Particularly, no report was focused on the indirect photochemical transformation mechanisms of tonalide, although a paper suggested that the indirect photo-transformation processes were important and more likely to occur, because various photochemically active light absorbers are present in surface waters (Fenner et al., 2013). In fact, indirect photochemical transformation of organics involves a number of reactive oxygen species (ROSs) such as •OH, $H_2O_2$ and $^1O_2$ (Dong and Rosario-Ortiz, 2012), which can also stimulate the degradation of target compounds in surface water. Among these ROSs, •OH shows the highest reactivity and plays an important role in the photodegradation of a wide spectrum of contaminants (Dong and Rosario-Ortiz, 2012; Wenk et al., 2011). Therefore, the study of the role played by •OH-initiated indirect photolysis is expected to help properly understand the photochemical mechanism of tonalide in natural waters.

To have a cost-effective and convenient approach, which does not involve any harm to animals for toxicological studies, computational calculation is frequently adopted to investigate the environmental, chemical, and biological processes at the molecular level (An et al., 2014; Gao et al., 2015, 2014b, 2016; Rusyn and Daston, 2010; Wang et al., 2011). In this work, the •OH-initiated photochemical transformation mechanism, kinetics and fate of tonalide in aquatic environments were systematically investigated using the density functional theory (DFT). Further, considering that toxic intermediates produced during the •OH-initiated photochemical transformation of most emerging organics in water are higher than their parental compounds, the potential ecotoxicity of this process was also assessed. The bioaccumulation effects and potential exposure risks to fish of tonalide (originally present) and transformation products were evaluated in detail using model calculations. The obtained theoretical data would supply good complements to better understand the photochemical transformation of PCMs and hence, would allow the readers to better estimate the potential exposure risks to organisms imposed by PCMs and their transformation products in aquatic environment.

## 2. Computational methods

### 2.1. Mechanism computation

All quantum chemical calculations in this work were carried out using the Gaussian 09 package (Frisch et al., 2009). The geometry optimization of the reactants, products, and transition states (*TS*) were performed using hybrid density functional M06-2X method (Zhao and Truhlar, 2008a,b) with 6-31 + G (d,p) basis set. It has been shown that M06-2X can give the best performance without increasing the computational time for the thermochemistry and kinetics calculations (Li et al., 2014; Zhao and Truhlar, 2008b). Therefore, it has successfully been applied to simulate the radical-initiated oxidation of organics in environmental studies (So et al., 2014). The solvent effect of water was considered by continuum solvation model 'SMD' (Marenich et al., 2009). To identify all stationary points as either minima (zero imaginary frequency) or *TS* (only one imaginary frequency), and to obtain the thermodynamic contributions, harmonic vibrational frequencies were calculated at the same level as of geometry optimization. The minimum energy pathway (MEP) was obtained using intrinsic reaction coordinate (IRC) theory to confirm that each *TS* accurately connected the reactant with the associated product. Since the kinetics calculations are sensitive to activation energy, a more flexible basis set 6-311 + G (3df,2p) was therefore employed to determine the single point energies. The profile of potential energy surface (PES) was also constructed at M062X/6-311 + G (3df,2p) level.

### 2.2. Kinetics computation

The reaction kinetics was calculated using transition-state theory (TST) after considering both solvent cage and diffusion-limited effects. The rate constants ($k$) are calculated using Eq. (1) described in early published references (Evans and Polanyi, 1935; Eyring, 1935; Galano and Alvarez-Idaboy, 2009):

$$k = \sigma \frac{k_B T}{h} \exp\left(\frac{-\Delta G^{\neq}}{RT}\right) \quad (1)$$

where $k_B$ and $h$ are the Boltzmann and Planck constants respectively; $\Delta G^{\neq}$ is the free energy barrier including the thermodynamic contribution correction; $\sigma$ represents the reaction path degeneracy, accounting for the number of equivalent reaction paths.

To simulate realistic solution, the solvent cage effect is included according to the correction proposed by Okuno (1997) and the expression used to correct Gibbs free energy as follows:

$$\Delta G_S^{FV} \cong \Delta G_S^0 - RT\left\{Ln\left[n10^{(2n-2)}\right] - (n-1)\right\} \quad (2)$$

where $n$ represents the molecularity of the reaction.

For the diffusion-limit reaction, the apparent rate constant ($k_{app}$) cannot be directly obtained from TST calculations. It is calculated using the Collins-Kimball theory (Collins and Kimball, 1949):

$$k_{app} = \frac{kk_D}{k + k_D} \quad (3)$$

where $k$ is the thermal rate constant, obtained from TST calculations (Eq. (1)), and $k_D$ is the steady-state Smoluchowski rate constant for an irreversible bimolecular diffusion-controlled reaction (Gao et al., 2014a).

### 2.3. Bioconcentration and ecotoxicity assessment

Fish typically serves as a target aquatic species for bioconcentration and ecotoxicity assessments in view of its importance as food for many species including humans along with the availability of standardized testing protocols (Zhao et al., 2008). The bioconcentration factors (BCF) of tonalide and its transformation products were estimated using the regression-based method BCFBAF v 3.01 (USEPA (U.S. Environmental Protection Agency), 2016). Their ecotoxicities to fish were assessed using the "ecological structure–activity relationships (ECOSAR)" program (ECOSAR, 2014). Herein, acute toxicity is expressed using $LC_{50}$ value (the concentration of tested pollutant leading to 50% dead fish). As for complex chemicals with multi-functional groups with more than one effect concentration (such as $LC_{50}$) available, the lowest toxicity value was chosen for the most conservative estimate to be considered as the precautionary principle.

## 3. Results and discussion

### 3.1. Reactants properties and optimized structures

The optimized structures of both reactants (tonalide and •OH) and the carbon atom numbers of tonalide are shown in Fig. 1. Tonalide, as a naphthalene derivative, contains a substituted cyclohexane (C) and a benzene ring (B) with an acetyl group, with a dihedral angle of −177 Å between benzene and cyclohexane rings. That is, tonalide has a nearly coplanar conformation. This kind of structure might impose toxicity to fish and other organisms by affecting the interaction of coplanar chemicals with target cells (Uhle et al., 1999).

Further, the calculated structural parameters and harmonic vibrational frequencies of the reactants were calculated at M062X level. As shown in Fig. 1 and Table S1, the calculated frequency of •OH radicals of 3724 $cm^{-1}$ matches very well with the available experimental value of 3738 $cm^{-1}$ (Chase, 1998), although it is slightly lower than the previous result (3857 $cm^{-1}$) calculated at MP2(full)/6-311G (d,p) level (Liu et al., 2004). Thus, the calculated structural parameters for the stationary points were reliable at M062X/6-31 + G (d,p) level.

### 3.2. Initial reaction mechanisms of tonalide with •OH

The •OH-initiated indirect photochemical transformation mechanisms of tonalide were modeled and summarized as three groups in Scheme S1.

(i) •OH-addition: either onto C atom of benzene ring ($R_{add}$B1–6) or onto carbonyl group ($R_{add}$B7).
(ii) H-abstraction by •OHfrom benzene ring ($R_{abs}$B2 and $R_{abs}$B5), cyclohexane ring ($R_{abs}$C3′ and $R_{abs}$C2′), methyl group ($R_{abs}$B8, B9 and $R_{abs}$C1′, C4′, C5′).
(iii) Single-electron transfer: from tonalide molecules to •OH ($R_{set}$).

For the completeness of transformation mechanisms in this work, electron transfer pathway is still considered, although it is not a common mechanism for •OH-initiated reactions (Fang et al., 2000). Fig. S1 presents the optimized geometries of involved *TSs* for all reaction pathways. Generally, different transformation pathways have a dissimilar probability to take place, although they occur in parallel. As such, to further understand tonalide transformation fate in water under •OH conditions, both transformation mechanisms and main transformation products were studied.

Table 1 presents the computed reaction energy (ΔG) and energy barrier ($\Delta G^{\neq}$) of each reaction pathway. The single-electron transfer pathway ($R_{set}$) is found to be an endothermic process with a positive ΔG (18.88 kcal $mol^{-1}$), while other pathways including all •OH-addition and H-abstraction pathways are exothermic processes with negative ΔG (−2.47 to −29.42 kcal $mol^{-1}$). Thus, the pathway of single-electron transfer from tonalide molecule to •OH is predicted to be less spontaneous than other exothermic pathways, and can be completely ruled out from tonalide transformation process. It can therefore be concluded that electron transfer reaction has a very low occurrence probability. The result was also observed experimentally during the •OH-initiated transformation of most emerging organics such as phthalates (An et al., 2014) and parabens (Fang et al., 2013). For •OH-addition pathways, the highest energy barrier ($\Delta G^{\neq}$) of 19.06 kcal $mol^{-1}$ was located in carbonyl–•OH–addition pathway ($R_{add}$B7) (Table 1), which was higher by at least 7.76 kcal $mol^{-1}$ than benzene–•OH–addition pathways ($R_{add}$B1–6). This suggests that carbonyl group is more difficult to be attacked by •OH than the benzene ring of tonalide. Further, the reactivity of unsaturated carbonyl group is lower than the benzene ring among various emerging organics. Among six benzene–•OH–addition pathways ($R_{add}$B1–6), the calculated $\Delta G^{\neq}$ of $R_{add}$B1 and $R_{add}$B5 were obtained as 8.00 and 8.47 kcal $mol^{-1}$, respectively. These values are lower by 1.36–4.38 kcal $mol^{-1}$ than the pathways $R_{add}$B2,3,4,6. These imply

**Table 1**
Energy barriers ($\Delta G^{\neq}$) and reaction enthalpies (ΔG) for the •OH-initiated transformation process of tonalide (kcal $mol^{-1}$).

| •OH-addition | | | H-abstraction | | |
|---|---|---|---|---|---|
| Pathways | $\Delta G^{\neq}$ | ΔG | Pathways | $\Delta G^{\neq}$ | ΔG |
| $R_{add}$B1 | 8.00 | −9.72 | $R_{abs}$B2 | 13.91 | −10.88 |
| $R_{add}$B2 | 9.83 | −8.61 | $R_{abs}$B5 | 13.36 | −11.57 |
| $R_{add}$B3 | 12.38 | −4.71 | $R_{abs}$B8 | 12.15 | −25.31 |
| $R_{add}$B4 | 11.30 | −8.14 | $R_{abs}$B9 | 10.75 | −29.42 |
| $R_{add}$B5 | 8.47 | −6.87 | $R_{abs}$C1′ | 10.30 | −20.12 |
| $R_{add}$B6 | 10.07 | −10.83 | $R_{abs}$C2′ | 9.32 | −24.26 |
| $R_{add}$B7 | 19.06 | −2.47 | $R_{abs}$C3′ | 8.53 | −27.28 |
| SET Pathway | | | $R_{abs}$C4′ | 9.28 | −24.26 |
| $R_{set}$ | 27.88 | 18.88 | $R_{abs}$C5′ | 9.25 | −22.04 |

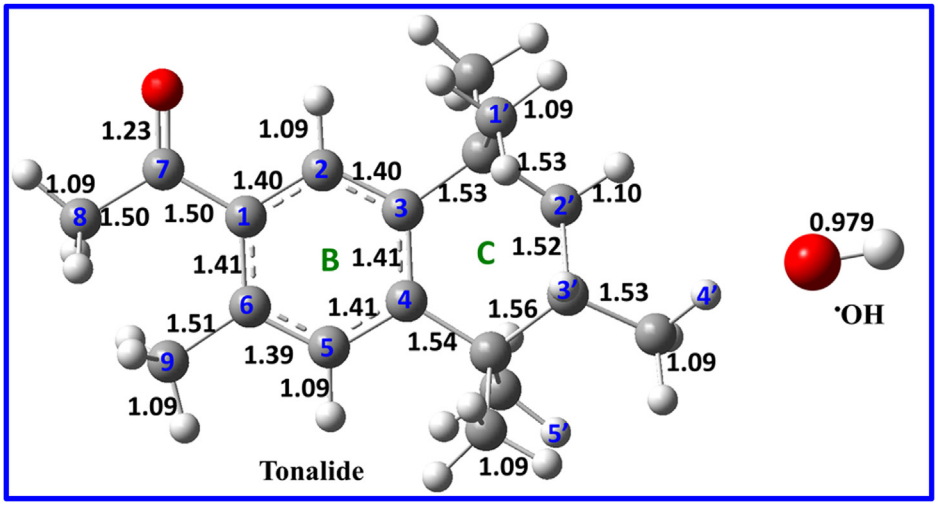


**Fig. 1.** The optimized geometries of reactants (tonalide and •OH) at the M062X/6–31 + g (d,p) level. Bond lengths are in angstroms (Å). ● = C, ● = H, ● = O.

that $R_{add}$B1 and $R_{add}$B5 pathways may be the most favorable •OH-addition pathways for tonalide transformation, leading to the formation of •OH-adducts of •tonalide-$OH_{B1}$ and •tonalide-$OH_{B5}$, respectively.

As for H-abstraction pathways, the $\Delta G^{\neq}$ of benzene−H−abstraction ($R_{abs}$B2 and $R_{abs}$B5) were 13.36 and 13.91 kcal $mol^{-1}$ respectively, which are higher by approximately 1.2–4.4 kcal $mol^{-1}$ than other H-abstraction pathways. This is due to lower reactivity of unsaturated benzene ring for H-abstraction reaction than the saturated cyclohexane ring and methyl group of tonalide. While for cyclohexane−H−abstraction pathway $R_{abs}$C3′, the calculated $\Delta G^{\neq}$ (8.53 kcal $mol^{-1}$) is the lowest among these H-abstraction pathways. That is, the former pathways ($R_{abs}$B2 and $R_{abs}$B5) can be ignored and the latter one ($R_{abs}$C3′) will be the most significant pathway. Nevertheless, due to small $\Delta G^{\neq}$ differences among other pathways ($R_{abs}$B8,9; $R_{abs}$C2′, and $R_{abs}$C1′,4′,5'), the contribution of different pathways is unlikely to be identified solely based on their mechanisms. Therefore, to distinguish each pathway, further kinetics calculation is still needed.

Based upon the above discussion, the single-electron transfer pathway ($R_{set}$), carbonyl−•OH−addition pathway ($R_{add}$B7), and two benzene-H-abstraction pathways ($R_{abs}$B2 and $R_{abs}$B5) can be ruled out from the •OH-initiated transformation pathways of tonalide due to the endothermic reactions or high energy barriers. Therefore, only six •OH-addition pathways ($R_{add}$B1–6) and seven H-abstraction pathways ($R_{abs}$C2′, C3′, and $R_{abs}$B8, B9, C1′, C4′, C5′) are found to be the important pathways and have been employed to assess the kinetics and products' toxicity.

### 3.3. Initial reaction kinetics of tonalide with •OH

To quantitatively evaluate the contribution of each pathway and provide detailed insights into the fate of tonalide in natural water, the •OH-initiated transformation rate constants of above mentioned 13 pathways were calculated within the temperature range of 273–313 K. The second-order rate constants of the tested pathways and total rate constant ($k_{total}$, the sum of rate constants of all these calculated pathways) were calculated. As shown in Table S2 and Fig. S2, the $k_{total}$ values fall into the range of $10^9$–$10^{10}$ $M^{-1}$ $s^{-1}$, which are close to the diffusion limited reaction over the whole temperature range ($4 \times 10^9$ $M^{-1}$ $s^{-1}$). This indicates that •OH-initiated photochemical transformation of tonalide is almost a diffusion-controlled process. Additionally, as in Fig. S2 and Table S2 show, the rate constants of all pathways and $k_{total}$ increased with the temperature. For example, $k_{total}$ increased from $6.03 \times 10^9$ to $1.58 \times 10^{10}$ $M^{-1}$ $s^{-1}$ as the temperature increased from 273 to 313 K. Thus, it can be concluded that increase of temperature promotes •OH-initiated transformation of tonalide. To some extent, this finding can explain the previously published experimental results that a pronounced seasonality of tonalide concentration is significantly correlated with water temperature (Buerge et al., 2003).

To further estimate the dependence of reaction kinetics upon temperature without experimental data, the Arrhenius formulae were established for the reactions within the temperature range of 273–313 K (Table S3). From the formulae, the activation energies of the reaction of tonalide with •OH was estimated to be only 4.11 kcal $mol^{-1}$ for the temperature range investigated. These indicate that tonalide is readily attacked by •OH in water.

The half-life ($t_{1/2}$) of tonalide •OH-initiated transformation was calculated using formula $t_{1/2} = \ln 2/(k_{total} \times [\bullet OH])$, where [•OH] is the •OH concentration of $10^{-12}$–$10^{-19}$ M in natural water (Allen et al., 1996; Brezonik and Fulkerson-Brekken, 1998; Burns et al., 2012). The $t_{1/2}$ decreased with increasing temperature at a fixed [•OH]. Similarly, $t_{1/2}$ decreased with increasing [•OH] at fixed temperature (Table S4). For instance, $t_{1/2}$ increased from 14.32 s to 4.22 y as [•OH] decreased from $4.0 \times 10^{-12}$ to $4.3 \times 10^{-19}$ M at 298 K. Notably, the $t_{1/2}$s are lower than the direct photolysis (4 h) of tonalide, as the [•OH] in natural surface water exceed $7.98 \times 10^{-15}$, $3.98 \times 10^{-15}$ and $3.04 \times 10^{-15}$ M at 273, 298, and 313 K, respectively. In these cases, tonalide will mainly be transformed through •OH-initiated indirect photochemical transformation process, rather than direct photolysis. Since these [•OH] are common in surface water, the transformation products and their environmental exposure risks during •OH-initiated indirect photochemical transformation of tonalide should be concerned seriously.

### 3.4. Prediction of primary transformation intermediates

To gain an understanding of the contribution of each pathway to the whole reaction and to quantitatively estimate the intermediates formed during the •OH-initiated transformation of tonalide, the dependence of branching ratio ($\Gamma$) upon temperature was calculated. Herein, $\Gamma$ of each pathway was determined using $\Gamma_i = \frac{k_i}{k_{total}}$, where $k_i$ is the reaction rate constant of $i$th pathway. The calculated $\Gamma$s within the temperature range of 273–313 K are summarized in Fig. 2.

For •OH-addition pathways, the $\Gamma$s for $R_{add}$B1 and $R_{add}$B5 pathways were obtained as 24.6% and 19.5% at 273 K, respectively, which are higher by at least 15% than the other four pathways. The $R_{add}$B1 and $R_{add}$B5 pathways remained the dominant pathways within whole temperature range of 213–313 K, although both of them decreased with increasing temperature. For example, at 313 K, $\Gamma$s were 14.5% ($R_{add}$B1) and 13.9% ($R_{add}$B5) are still higher by approximately 4% than the corresponding values of other pathways. Therefore, •tonalide-$OH_{B1}$ and •tonalide-$OH_{B5}$ adducts, are predicted to be the mainly formed intermediates through •OH-addition pathways.

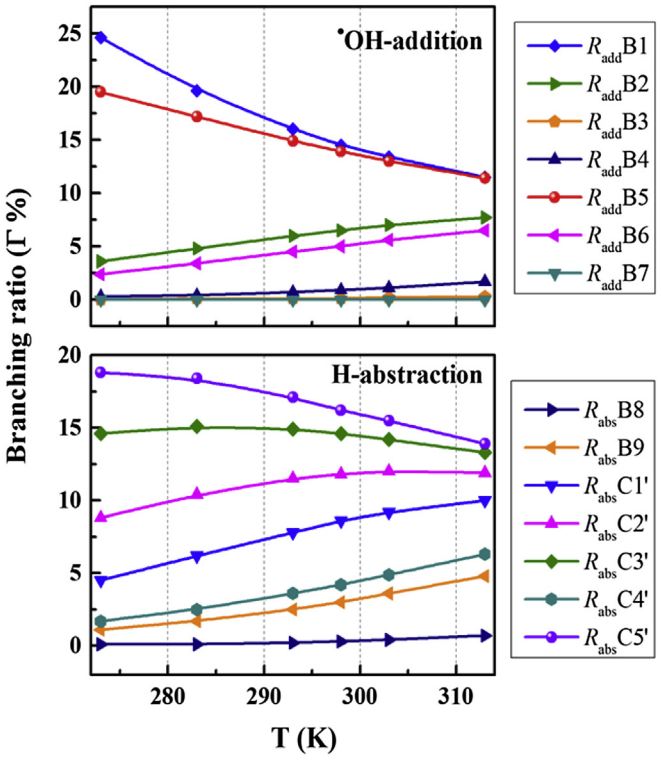


**Fig. 2.** Calculated branching ratios (Γ) of the main transformation pathways for the reaction of tonalide with •OH within the temperature range of 273–313 K.

For H-abstraction pathways, the contribution of the methyl-H-abstraction pathway ($R_{abs}$B8) was found to be less than 0.7% of total rate constant within the temperature range investigated. This indicates that this pathway can be completely ignored especially at low temperatures. However, $\Gamma$s for $R_{abs}$C5′ and $R_{abs}$C3′ pathways were 18.8% and 14.6% respectively at 273 K. Other H-abstraction pathways contributed 4.5% ($R_{abs}$C1′), 8.8% ($R_{abs}$C2′), 1.7% ($R_{abs}$C4′) and 1.1% ($R_{abs}$ B9) to the total rate constant. The contribution of $R_{abs}$C5′ and $R_{abs}$C3′ pathways decreased to 13.9%–13.3% at 313 K, although both pathways remained the dominant. Therefore, the dehydrogenized intermediates •tonalide $(-H)_{C5'}$ and •tonalide $(-H)_{C3'}$ are found to be the main intermediates formed through H-abstraction pathways.

In sum, two •OH-addition pathways ($R_{add}$B1 and $R_{add}$B5) and two H-abstraction pathways ($R_{abs}$C3′ and $R_{abs}$C5′) would be the main pathways for tonalide transformation in water, producing the •OH-addition and H-abstraction intermediates. These two kinds of transient intermediates can be further confirmed by recent experimental study (Fang et al., 2016), and their transient absorption spectra were also observed at 450 and 360 nm, respectively. Among them, •OH-addition pathways are found more important than H-abstraction at low temperatures (<~287 K) (Fig. S3). Particularly, $R_{add}$B1 is the most dominated pathway, mainly producing •OH-adduct •tonalide-$OH_{B1}$. With increasing temperature, the role of •OH-addition pathways became less significant. At 313 K, H-abstraction pathways was found to be dominant to form the dehydrogenized intermediates (•tonalide $(-H)_{C5'}$ and •tonalide $(-H)_{C3'}$).

### 3.5. Formation of primary transformation products

Results discussed above show that several intermediates including •OH-adducts (•tonalide-$OH_{B1}$ and •tonalide-$OH_{B5}$) and dehydrogenated radicals (•tonalide $(-H)_{C5'}$ and •tonalide $(-H)_{C3'}$) can be produced as the dominant intermediates in the initial reactions of tonalide with •OH. These intermediates, acting as highly activated radicals, can further undergo a series of reactions to produce more stable transformation products. Therefore, the subsequent reactions of these primary intermediates are necessary to be further tracked.

*•OH-addition Intermediates.* The subsequent degradation pathways of intermediate •tonalide-$OH_{B1}$ were calculated. As Fig. 3a–c shows, the released energy of the former step of •tonalide-$OH_{B1}$ is only 9.72 kcal mol$^{-1}$, which is not enough to support •tonalide-$OH_{B1}$ to undergo the ring-opening reaction ($\Delta G^{\neq}$ = 35.93 kcal mol$^{-1}$). That is, the ring-opening reaction of •tonalide-$OH_{B1}$ is difficult to occur through intramolecular H-transfer of •tonalide-$OH_{B1}$, and therefore can be ruled out. However, •tonalide-$OH_{B1}$ can directly undergo the cleavage of C–C bond linking carbonyl group and benzene ring (Fig. 3a), leading to the formation of acetaldehyde radical ($CH_3$(C=O)•) and phenolic product (PC1) due to this process only needs to overcome $\Delta G^{\neq}$ of 3.42 kcal mol$^{-1}$, which is lower by at least 30 kcal mol$^{-1}$ than the former ring-opening reaction. As a result, acetaldehyde radical ($CH_3$(C=O)•) and phenolic product (PC1) should be obtained as the main transformation products in the •OH-initiated indirect photochemical transformation.

Under certain conditions with enough •OH such as in surface water receiving acidic mine drainage runoff (Allen et al., 1996), Lake Nichols in northern Wisconsin (Brezonik and Fulkerson-Brekken, 1998), and advanced oxidation processes (Fig. 3b), •tonalide-$OH_{B1}$ was more susceptible to be attacked by •OH to form three dihydroxyl isomers ($OH_{B1}$-$OH_{B2,4,6}$). This is due to that these three reactions were barrier-less processes with very strong exothermic energies of −70.65, −66.36 and −67.84 kcal mol$^{-1}$, respectively. Additionally, the released energies are more than the energy barriers of the subsequent reactions (43.30, 38.32 and 44.40 kcal mol$^{-1}$), to form phenolic product (PC1), ketone product (PC2) and acetic acid. Similar conclusion can be drawn for the subsequent transformation pathways of •tonalide-$OH_{B5}$ (Fig. S4a). That is, it would also be easily converted to dihydroxyl isomers including $OH_{B5}$-$OH_{B2}$, $OH_{B5}$-$OH_{B4}$ and $OH_{B5}$-$OH_{B6}$. These products could be further transformed to monohydroxylated product tonalide-$OH_{B5}$ via $H_2O$-elimination process. Overall, dihydroxyl isomers ($OH_{B1}$-$OH_{B2,4,6}$ and $OH_{B5}$-$OH_{B2,4,6}$), monohydroxylated product (tonalide-$OH_{B5}$), PC1, PC2, and acetic acid were the main transformation products in the presence of •OH. These identified hydroxylated products were also detected in our previously published experimental work (Fang et al., 2016). This further confirmed the correction of our calculated transformation mechanism. Moreover, this theoretical result would shed light on the formation pathways of transformation products in the experiment and the attack position by •OH.

$O_2$ is a mild oxidant and might participate in the subsequent tonalide transformation reaction in aerated water. Therefore, to better understand the subsequent fate of tonalide, the presence of $O_2$ in the reaction was also considered. As Fig. 3c shows, •tonalide-$OH_{B1}$ can easily react with $O_2$ through an endothermic process with $\Delta G^{\neq}$ = 5.68 kcal mol$^{-1}$, producing intermediate (IM2). By further comparing the subsequent transformation of IM2, the $\Delta G^{\neq}$ of H-transfer pathway ($TS7_{H\text{-}transfer}$) was found to be 11.81 kcal mol$^{-1}$, which is lower by approximately 7.2 kcal mol$^{-1}$ than the opening-ring pathway ($TS6_{opening\text{-}ring}$). This suggests that the former pathway was easier to occur than the latter, and IM2 can be further degraded into quinone product (PC3), acetaldehyde and •OH. This finding could theoretically reveal the photochemical formation of •OH from the emerging organics in natural waters.

Similar conclusion can be drawn for the subsequent transformation pathways of •tonalide-$OH_{B5}$ (Fig. S4b). Monohydroxylated product (tonalide-$OH_{B5}$), dihydroxylated product (PC4) and several ROSs including •OH and peroxy radical (•OOH) were the main transformation products in the •OH-initiated indirect photochemical transformation process. The resultant ROSs will further promote tonalide photochemical transformation in natural waters.

*H-abstraction Intermediate.* The subsequent transformation pathway of H-abstraction intermediate •tonalide $(-H)_{C5'}$ was also investigated (Fig. S5). •tonalide $(-H)_{C5'}$ is prone to be further attacked by •OH in the presence of enough [•OH], to produce a stable alcohol product (PC5). This is because that this process is barrier-less and strongly exothermic process with a release energy of −102.17 kcal mol$^{-1}$, which is enough to completely overcome the later demethanation reaction with energy barrier of 75.76 kcal mol$^{-1}$. Then the main transformation product, aldehyde derivative (PC6), will be formed. Similar conclusion can be drawn for the subsequent transformation pathways of •tonalide $(-H)_{C3'}$ (Fig. S6), during which the alcohol (PC8) and aldehyde (PC9) are also formed.

Similarly, in aerated water, the reaction of $O_2$ at the methene group of •tonalide $(-H)_{C5'}$ could form the peroxyl radical ((tonalide-H)-OO•) (Fig. S5) via a barrier-less process with an exothermic energy of −46.46 kcal mol$^{-1}$. Then (tonalide-H)-OO• could transform into stable PC7 with an energy barrier of 41.15 kcal mol$^{-1}$ along with •OH formation. In case of •tonalide $(-H)_{C3'}$(Fig. S6), a similar product (PC9) is mainly formed by eliminating the methoxyl radical from •tonalide $(-H)_{C5'}$.

In short, during the •OH-initiated indirect photochemical transformation process of tonalide, different transformation products would be formed through •OH-addition and H-abstraction pathways, as well as possible subsequent reactions. For •OH-

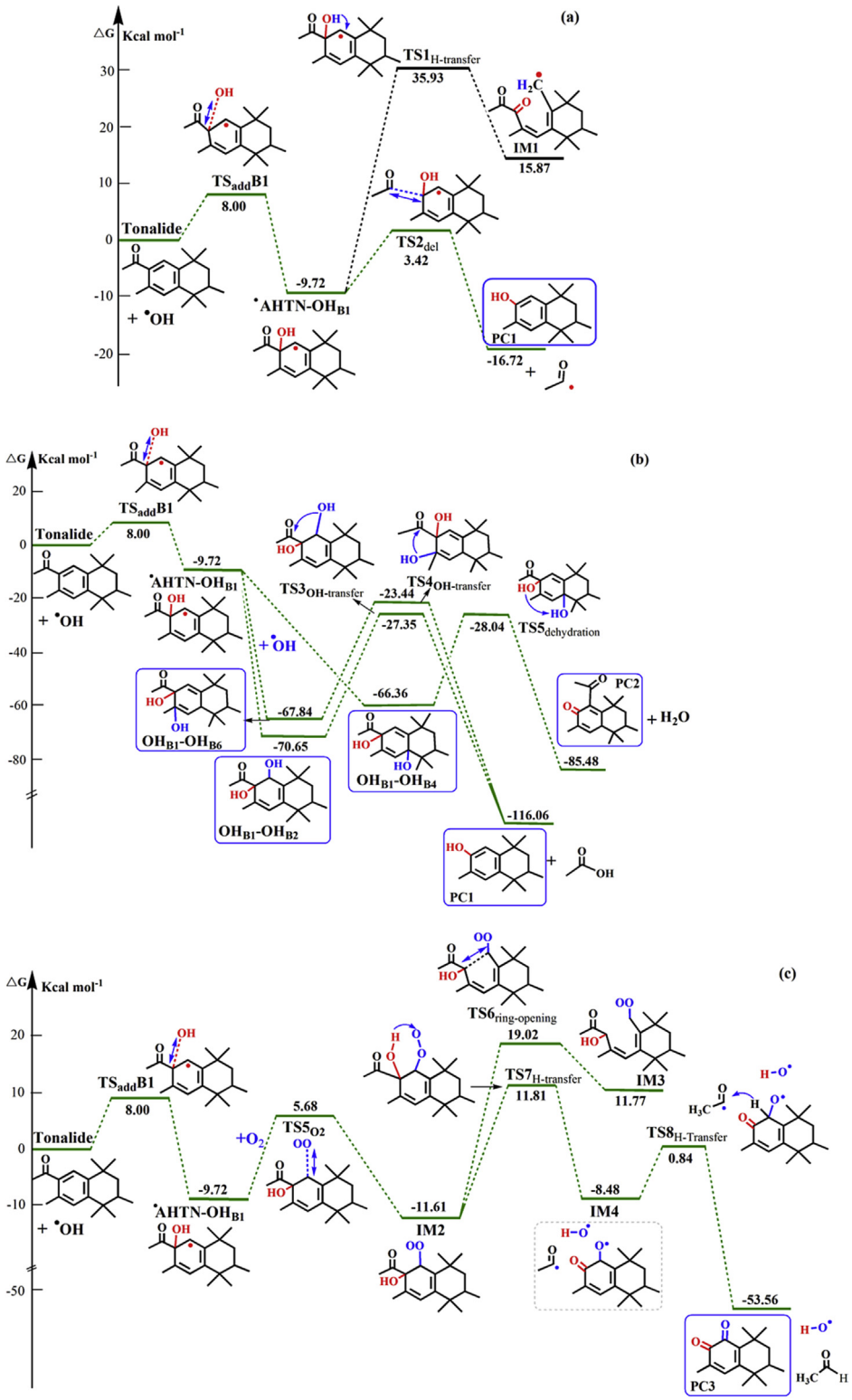


**Fig. 3.** Schematic diagram of the subsequent pathways of •tonalide-$OH_{B1}$. a: with insufficient •OH; b: with enough •OH; c: with $O_2$.

addition pathways, the phenolic products (PC1, PC4 and tonalide-$OH_{B5}$), benzoquinone derivatives (PC2 and PC3), dihydroxyl products ($OH_{B1}$-$OH_{B2,4,6}$ and $OH_{B5}$-$OH_{B2,4,6}$), and other small molecular products like •OH and acetic acid would mainly be formed. While for H-abstraction intermediates, alcohols (PC5 and PC8) and aldehydes (PC6, PC7 and PC9) were obtained as the main transformation products.

### 3.6. Bioaccumulation assessment for tonalide and its transformation products

The documented high concentration of tonalide in biota

indicated its potential bioaccumulation in aquatic organisms (Fromme et al., 2001b). Therefore, the bioaccumulation of tonalide in fish was assessed by calculating BCF, which is the most commonly used indicator for the ability of chemicals to accumulate in aquatic organisms (Meylan et al., 1999). Furthermore, to answer the questions whether the formed products have the potential bioaccumulation during the •OH-initiated indirect photochemical transformation of tonalide in water and whether they will tend to accumulate more in aquatic organisms than original tonalide, the BCF of the transformation products were estimated. Generally, higher values of BCF of organics indicate higher bioaccumulation potential in fish tissue (Abhilash et al., 2009). According to REACH Annex XIII (2011) (Fernandez et al., 2012) and the Toxic Substances Control Act (TSCA) of United States (Conder et al., 2008), a compound with 1 < BCF<1000 was labeled as "tendency to accumulate in organisms"; 1000 < BCF<5000 as "bioaccumulative (B)"; and BCF >5000 as "very bioaccumulative (VB)" (Table S5). As shown in Tables S6–S8, the BCF of tonalide (696 L/kg wet-wt) is well comparable to the experimental data for Crucian carp (670 L/kg wet-wt) and zebrafish (600 L/kg wet-wt) (Gatermann et al., 2002; Rimkus, 1999). These high BCF values mean a significant bioaccumulation potential of tonalide to fish.

For the transformation products of $R_{add}B_1$ pathway (Table S6 and Fig. 4), lower BCF of $OH_{B1}$-$OH_{B4}$ (145 L/kg wet-wt) indicates lower bioaccumulation propensity than tonalide in fish. However, higher BCFs (899–5590 L/kg wet-wt) of the rest of transformation products (PC1- PC3, and $OH_{B1}$-$OH_{B2,\ 6}$) of $R_{add}B1$ pathway were also observed. These indicate that all these products would tend to bioaccumulate in fish during indirect photolysis of tonalide transformation (Fig. 4). According to Tables S5 and S6, three indirect photolysis products ($OH_{B1}$-$OH_{B2}$, PC2, and PC3) with BCFs of 1744, 2016, and 1538 L/kg wet-wt respectively are considered to be "bioaccumulative", suggesting their high occurrence in water. Particularly, the phenolic product PC1 with an extremum high BCF (5590 L/kg wet-wt) was identified as "very bioaccumulative". The value slightly exceeds the cutoff criterion (5000 L/kg wet-wt) set for the typically persistent organics, and therefore is termed as critically bioaccumulative (Holbrook et al., 2008). Based on the obtained transformation mechanisms, it is found that the presence of $O_2$ or warm water environments will be unfavorable to form PC1. Thus, during the •OH-initiated indirect photolysis, this critically bioaccumulative product PC1 should be paid more attention in cold water environments or under the anaerobic conditions.

However, various bioaccumulation assessment results were obtained for $R_{add}B5$ pathway (Fig. S7 and Table S7). The product PC4 formed in the aerated aquatic environment would tend to bioaccumulate in fish through pathway $R_{add}B5$, due to its higher BCF (842 L/kg wet-wt). Compared with tonalide, other products have lower bioaccumulation ability (Fig. S7 and Table S6), although they would be potentially bioaccumulated in fish. This theoretical results reveal that aquatic organisms could suffer more serious impact during the •OH-initiated indirect photochemical transformation in water, due to the accumulation of these transformation products.

As for H-abstraction pathways (Table S8 and Figs. S8–S9), the BCFs of all transformation products were in the range of 44–189 L/kg wet-wt, which are 3–15 times lower than that of tonalide. This indicates that the bioaccumulation of all these H-abstraction products is less than tonalide, and would be insignificant during the •OH-initiated indirect photochemical transformation of tonalide.

### 3.7. Aquatic toxicity of tonalide and its transformation products

Above results suggest that, during indirect photochemical transformation of tonalide, some products can potentially bioaccumulate in fish, indicating an increase of risks to aquatic organisms. In this study, the acute and chronic toxicities of tonalide as well as its transformation products to fish were estimated using ECOSAR program. As shown in Fig. 5 and Tables S6–S8, the acute ($LC_{50}$) and chronic toxicity values (ChV) of tonalide were obtained as 0.10 and 0.02 mg $L^{-1}$, respectively. According to the European Union criteria (described in Annex VI of Directive 67/548/EEC) and the Chinese hazard evaluation guidelines for new chemicals (HJ/T 154–2004) (Table S9), tonalide is classified as very toxic to fish ($LC_{50}$ < 1.0 mg $L^{-1}$ and ChV<0.1 mg $L^{-1}$) both acute and chronic toxicities. Therefore, the aquatic toxicity of tonalide transformation products during •OH-initiated indirect photochemical transformation process should be considered.

Fig. 5 and Fig. S10 shows the aquatic toxicity evolution through •OH-addition transformation pathways $R_{add}B1$ and $R_{add}B5$. Tables S6–S7 also list the corresponding toxic values. The $LC_{50}$ of the phenolic products (PC1 and tonalide-$OH_{B5}$) were obtained as 0.03 and 0.06 mg $L^{-1}$ respectively, which are approximately 3 and 1.7 times lower than that of tonalide. This suggests that the acute toxicity would be increased during tonalide transformation to PC1 and tonalide-$OH_{B5}$. However, smaller acute toxicity were found in the formation of all other transformation products (PC2, PC3, $OH_{B1}$-$OH_{B2,4,6}$ and $OH_{B5}$-$OH_{B2,4,6}$), although they have the same toxic level as tonalide, except the acute toxicity of $OH_{B1}$-$OH_{B4}$ ($LC_{50}$ = 2.83 mg $L^{-1}$), which is classified as less toxic by one level.

For chronic toxicity, the ChVs for all formed products except PC1,

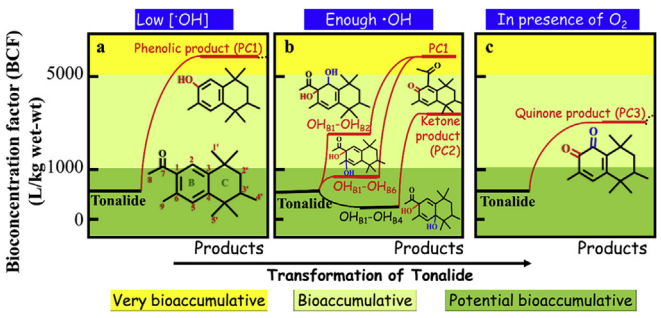


**Fig. 4.** Bioaccumulation assessment of transformation products through $R_{add}B1$ pathway. Dihydroxyl products were denoted as "$OH_n$-$OH_m$", and the subscript n and m denoted the position of OH group in benzene ring of tonalide.

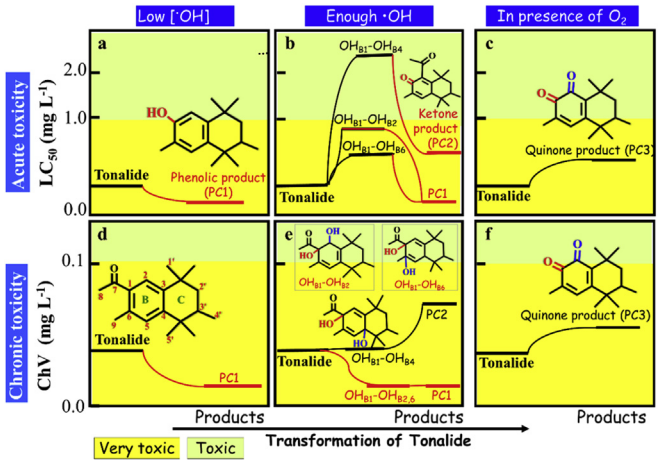


**Fig. 5.** Evolution of acute and chronic toxicities to fish through $R_{add}B1$ transformation pathway. Dihydroxyl products were denoted as "$OH_n$-$OH_m$", and the subscript n and m denoted the position of OH group in benzene ring of tonalide.

PC4, $OH_{B1}$-$OH_{B2,6}$ and tonalide-$OH_{B5}$, were either same or larger than that of tonalide (0.02 mg $L^{-1}$). This suggests that chronic toxicity to fish would increase during these products (PC1, PC4, $OH_{B1}$-$OH_{B2,6}$ and tonalide-$OH_{B5}$) formation. The toxicity evolution would always be the same for the transformation of dihydroxylated products ($OH_{B1}$-$OH_{B2}$ and $OH_{B1}$-$OH_{B6}$) to PC1 (Fig. 5). This finding well explains the experimental facts that prolonged irradiation or ozonation bring no reduction of tonalide toxicity (Santiago-Morales et al., 2012).

However, different results were obtained through the H-abstraction pathways $R_{abs}$C5′ and $R_{abs}$C3' (Figs. S11–S12). The acute and chronic toxicities would decrease during tonalide transformation through both mentioned ($R_{abs}$C5′ and $R_{abs}$C3') pathways. But nearly all transformation products were still identified as very toxic, and showed at the same toxic level as that of tonalide. Therefore, these H-abstraction products should not be neglected during such an analysis.

Thus, it can be concluded that, during the •OH-initiated indirect photochemical transformation of tonalide in water, all H-abstraction products possessed lower aquatic toxicity, while the •OH-addition products including phenolic products (PC1 and tonalide-$OH_{B5}$) exhibited higher aquatic toxicity than tonalide. Theoretical results further revealed the reason of experimental speculation from the viewpoint of organics (Parolini et al., 2015). Namely, the aquatic organisms, which are exposed to tonalide for their entire life span, possible result in high toxicity. Thus, the aquatic toxicity of these indirect photochemical transformation products and tonalide should not be ignored.

## 4. Conclusions

This paper theoretically evaluated the •OH-initiated indirect photochemical transformation of typical polycyclic musk tonalide. The photochemical transformation mechanisms, kinetics, bioaccumulation and ecotoxicities of transformation products to fish were investigated. The major findings are listed as following:

1) •OH-initiated indirect photochemical transformation plays an important role in tonalide photochemical degradation in aquatic environment. Particularly, it would be more important than direct photochemical transformation, as [•OH] exceeds $7.98 \times 10^{-15}$ M.
2) The environment temperature can significantly influence tonalide transformation mechanism. For example, •OH-addition pathway was dominant at low temperature, whereas H-abstraction will be predominant at high temperature.
3) Compared with tonalide, all the transformation products from H-abstraction were less bioaccumulative and less toxic to fish, but most of the transformation products from •OH-addition have up to 8 times higher BCF and severer aquatic toxicity, during the •OH-initiated indirect photochemical transformation process of tonalide.
4) The most bioaccumulative and toxic product were mainly formed under anaerobic or low temperatures aquatic conditions, during the •OH-initiated indirect photochemical transformation process of tonalide.
5) The environmental impact of PCMs and their degradation products in water should be paid more attention in the future experimental studies and environmental assessment.

## Acknowledgments

Authors appreciate the financial supports from National Natural Science Funds for Distinguished Young Scholars (41425015), National Natural Science Foundation of China (41603115), Science and Technology Project of Guangdong Province, China (2016A030310120) and China Postdoctoral Science Foundation (2015M572375).

## Appendix A. Supplementary data

Supplementary data related to this article can be found at http://dx.doi.org/10.1016/j.watres.2016.08.055.

## References

Abhilash, P.C., Pandey, V.C., Srivastava, P., Rakesh, P.S., Chandran, S., Singh, N., Thomas, A.P., 2009. Phytofiltration of cadmium from water by *Limnocharis flava* (L.) Buchenau grown in free-floating culture system. J. Hazard. Mater. 170, 791–797.

Allen, J.M., Lucas, S., Allen, S.K., 1996. Formation of hydroxyl radical ((OH)-O-center dot) in illuminated surface waters contaminated with acidic mine drainage. Environ. Toxicol. Chem. 15, 107–113.

An, T.C., Gao, Y.P., Li, G.Y., Kamat, P.V., Peller, J., Joyce, M.V., 2014. Kinetics and mechanism of (OH)-O-center dot mediated degradation of dimethyl phthalate in aqueous solution: experimental and theoretical studies. Environ. Sci. Technol. 48, 641–648.

Brezonik, P.L., Fulkerson-Brekken, J., 1998. Nitrate-induced photolysis in natural waters: controls on concentrations of hydroxyl radical photo-intermediates by natural scavenging agents. Environ. Sci. Technol. 32, 3004–3010.

Buerge, I.J., Buser, H.R., Muller, M.D., Poiger, T., 2003. Behavior of the polycyclic musks HHCB and AHTN in lakes, two potential anthropogenic markers for domestic wastewater in surface waters. Environ. Sci. Technol. 37, 5636–5644.

Burns, J.M., Cooper, W.J., Ferry, J.L., King, D.W., DiMento, B.P., McNeill, K., Miller, C.J., Miller, W.L., Peake, B.M., Rusak, S.A., Rose, A.L., Waite, T.D., 2012. Methods for reactive oxygen species (ROS) detection in aqueous environments. Aquat. Sci. 74, 683–734.

Chase, M.W., 1998. NIST-JANAF thermochemical tables, Monograph 9, fourth ed., Journal of physical and chemical reference data.

Chase, D.A., Karnjanapiboonwong, A., Fang, Y., Cobb, G.P., Morse, A.N., Anderson, T.A., 2012. Occurrence of synthetic musk fragrances in effluent and non-effluent impacted environments. Sci. Total Environ. 416, 253–260.

Chen, G.S., Jiang, R.F., Qiu, J.L., Cai, S.Y., Zhu, F., Ouyang, G.F., 2015. Environmental fates of synthetic musks in animal and plant: an in vivo study. Chemosphere 138, 584–591.

Clara, M., Gans, O., Windhofer, G., Krenn, U., Hartl, W., Braun, K., Scharf, S., Scheffknecht, C., 2011. Occurrence of polycyclic musks in wastewater and receiving water bodies and fate during wastewater treatment. Chemosphere 82, 1116–1123.

Collins, F.C., Kimball, G.E., 1949. Diffusion-controlled reaction rates. J. Colloid Sci. 4 (4), 425–437.

Conder, J.M., Hoke, R.A., Wolf, W.d., Russell, M.H., Buck, R.C., 2008. Are PFCAs bioaccumulative? a critical review and comparison with regulatory criteria and persistent lipophilic compounds. Environ. Sci. Technol. 42, 995–1003.

Dong, M.M., Rosario-Ortiz, F.L., 2012. Photochemical formation of hydroxyl radical from effluent organic matter. Environ. Sci. Technol. 46, 3788–3794.

ECOSAR (2014) http://www.epa.gov/oppt/newchems/tools/21ecosar.htm.

Evans, M.G., Polanyi, M., 1935. Some applications of the transition state method to the calculation of reaction velocities, especially in solution. Trans. Faraday Soc. 31 (1), 875–893.

Eyring, H., 1935. The activated complex in chemical reactions. J. Chem. Phys. 3 (2), 107–115.

Fang, X.W., Schuchmann, H.P., von Sonntag, C., 2000. The reaction of the OH radical with pentafluoro-, pentachloro-, pentabromo- and 2,4,6-triiodophenol in water: electron transfer vs. addition to the ring. J. Chem. Soc. Perkin Trans. 2, 1391–1398.

Fang, H.S., Gao, Y.P., Li, G.Y., An, J.B., Wong, P.K., Fu, H.Y., Yao, S.D., Nie, X.P., An, T.C., 2013. Advanced oxidation kinetics and mechanism of preservative propylparaben degradation in aqueous suspension of $TiO_2$ and risk assessment of its degradation products. Environ. Sci. Technol. 47, 2704–2712.

Fang, H.S., Li, G.Y., Yao, S.D., Liang, X.M., An, T.C., 2016. Kinetic and mechanism studies of musk tonalide reacted with hydroxyl radical and the risk assessment of degradation products. Catal. Today. http://dx.doi.org/10.1016/j.cattod.2016.06.021.

Fenner, K., Canonica, S., Wackett, L.P., Elsner, M., 2013. Evaluating pesticide degradation in the environment: blind spots and emerging opportunities. Science 341, 752–758.

Fernandes, D., Dimastrogiovanni, G., Blazquez, M., Porte, C., 2013. Metabolism of the polycyclic musk galaxolide and its interference with endogenous and xenobiotic metabolizing enzymes in the European sea bass (Dicentrarchus labrax). Environ. Pollut. 174, 214–221.

Fernandez, A., Lombardo, A., Rallo, R., Roncaglioni, A., Giralt, F., Benfenati, E., 2012. Quantitative consensus of bioaccumulation models for integrated testing strategies. Environ. Int. 45, 51–58.

Frisch, M.J., Trucks, G.W., Schlegel, H.B., Scuseria, G.E., Robb, M.A., Cheeseman, J.R., Scalmani, G., Barone, V., Mennucci, B., Petersson, G.A., Nakatsuji, H., Caricato, M.,

Li, X., Hratchian, H.P., Izmaylov, A.F., Bloino, J., Zheng, G., Sonnenberg, J.L., Hada, M., Ehara, M., Toyota, K., Fukuda, R., Hasegawa, J., Ishida, M., Nakajima, T., Honda, Y., Kitao, O., Nakai, H., Vreven, T., Montgomery Jr., J.A., Peralta, J.E., Ogliaro, F., Bearpark, M.J., Heyd, J., Brothers, E.N., Kudin, K.N., Staroverov, V.N., Kobayashi, R., Normand, J., Raghavachari, K., Rendell, A.P., Burant, J.C., Iyengar, S.S., Tomasi, J., Cossi, M., Rega, N., Millam, N.J., Klene, M., Knox, J.E., Cross, J.B., Bakken, V., Adamo, C., Jaramillo, J., Gomperts, R., Stratmann, R.E., Yazyev, O., Austin, A.J., Cammi, R., Pomelli, C., Ochterski, J.W., Martin, R.L., Morokuma, K., Zakrzewski, V.G., Voth, G.A., Salvador, P., Dannenberg, J.J., Dapprich, S., Daniels, A.D., Farkas, Ö., Foresman, J.B., Ortiz, J.V., Cioslowski, J., Fox, D.J., 2009. Gaussian 09. Gaussian, Inc., Wallingford, CT, USA.

Fromme, H., Otto, T., Pilz, K., 2001a. Polycyclic musk fragrances in different environmental compartments in Berlin (Germany). Water Res. 35, 121–128.

Fromme, H., Otto, T., Pilz, K., 2001b. Polycyclic musk fragrances in fish samples from Berlin waterways, Germany. Food Addit. Contam. 18, 937–944.

Galano, A., Alvarez-Idaboy, J.R., 2009. Guanosine plus OH radical reaction in aqueous solution: a reinterpretation of the UV-vis data based on thermodynamic and kinetic calculations. Org. Lett. 11 (22), 5114–5117.

Gao, Y.P., An, T.C., Fang, H.S., Ji, Y.M., Li, G.Y., 2014a. Computational consideration on advanced oxidation degradation of phenolic preservative, methylparaben, in water: mechanisms, kinetics, and toxicity assessments. J. Hazard. Mater 278, 417–425.

Gao, Y.P., Ji, Y.M., Li, G.Y., An, T.C., 2014b. Mechanism, kinetics and toxicity assessment of OH-initiated transformation of triclosan in aquatic environments. Water Res. 49, 360–370.

Gao, Y.P., An, T.C., Ji, Y.M., Li, G.Y., Zhao, C.Y., 2015. Eco-toxicity and human estrogenic exposure risks from OH-initiated photochemical transformation of four phthalates in water: a computational study. Environ. Pollut. 206, 510–517.

Gao, Y.P., Ji, Y.M., Li, G.Y., An, T.C., 2016. Theoretical investigation on the kinetics and mechanisms of hydroxyl radical-induced transformation of parabens and its consequences for toxicity: influence of alkyl-chain length. Water Res. 91, 77–85.

Gatermann, R., Biselli, S., Huhnerfuss, H., Rimkus, G.G., Hecker, M., Karbe, L., 2002. Synthetic musks in the environment. Part 1: species-dependent bioaccumulation of polycyclic and nitro musk fragrances in freshwater fish and mussels. Archives Environ. Contam. Toxicol. 42, 437–446.

Gómez, M.J., Herrera, S., Solé, D., García-Calvo, E., Fernández-Alba, A.R., 2012. Spatio-temporal evaluation of organic contaminants and their transformation products along a river basin affected by urban, agricultural and industrial pollution. Sci. Total Environ. 420, 134–145.

Heberer, T., 2003. Occurrence, fate, and assessment of polycyclic musk residues in the aquatic environment of urban areas - a review. Acta hydroch. Hydro. 30, 227–243.

Holbrook, R.D., Murphy, K.E., Morrow, J.B., Cole, K.D., 2008. Trophic transfer of nanoparticles in a simplified invertebrate food web. Nat. Nanotechnol. 3, 352–355.

Kannan, K., Reiner, J.L., Yun, S.H., Perrotta, E.E., Tao, L., Johnson-Restrepo, B., Rodan, B.D., 2005. Polycyclic musk compounds in higher trophic level aquatic organisms and humans from the United States. Chemosphere 61, 693–700.

Lange, C., Kuch, B., Metzger, J.W., 2015. Occurrence and fate of synthetic musk fragrances in a small German river. J. Hazard. Mater. 282, 34–40.

Li, C., Xie, H.B., Chen, J.W., Yang, X.H., Zhang, Y.F., Qiao, X.L., 2014. Predicting gaseous reaction rates of short chain chlorinated paraffins with center dot OH: overcoming the difficulty in experimental determination. Environ. Sci. Technol. 48, 13808–13816.

Liu, J.Y., Li, Z.S., Dai, Z.W., Zhang, G., Sun, C.C., 2004. Dual-level direct dynamics studies for the hydrogen abstraction reaction of 1,1-difluoroethane with O(P-3). Chem. Phys. 296, 43–51.

Lu, B.Y., Feng, Y.J., Gao, P., Zhang, Z.H., Lin, N., 2015. Distribution and fate of synthetic musks in the Songhua River, Northeastern China: influence of environmental variables. Environ. Sci. Pollut. Res. 22 (12), 9090–9099.

Luckenbach, T., Epel, D., 2005. Nitromusk and polycyclic musk compounds as long-term inhibitors of cellular xenobiotic defense systems mediated by multidrug transporters. Environ. Health Persp. 113, 17–24.

Marenich, A.V., Cramer, C.J., Truhlar, D.G., 2009. Universal solvation model based on solute electron density and on a continuum model of the solvent defined by the bulk dielectric constant and atomic surface tensions. J. Phys. Chem. B 113, 6378–6396.

Meylan, W.M., Howard, P.H., Boethling, R.S., Aronson, D., Printup, H., Gouchie, S., 1999. Improved method for estimating bioconcentration/bioaccumulation factor from octanol/water partition coefficient. Environ. Toxicol. Chem. 18, 664–672.

Okuno, Y., 1997. Theoretical investigation of the mechanism of the baeyer-villiger reaction in nonpolar solvents. Chem. – Eur. J. 3 (2), 210–218.

Parolini, M., Magni, S., Traversi, I., Villa, S., Finizio, A., Binelli, A., 2015. Environmentally relevant concentrations of galaxolide (HHCB) and tonalide (AHTN) induced oxidative and genetic damage in Dreissena polymorpha. J. Hazard. Mater. 285, 1–10.

Rimkus, G.G., 1999. Polycyclic musk fragrances in the aquatic environment. Toxicol. Lett. 111, 37–56.

Rusyn, I., Daston, G.P., 2010. Computational toxicology: realizing the promise of the toxicity testing in the 21st century. Environ. Health Persp. 118, 1047–1050.

Sanchez-Prado, Lucía, Lourido, M., Lores, M., Llompart, M., Garcia-Jares, C., Cela, R., 2004. Study of the photoinduced degradation of polycyclic musk compounds by solid-phase microextraction and gas chromatography/mass spectrometry. Rapid Commun. Mass Spectrom. 18, 1186–1192.

Santiago-Morales, J., Gomez, M.J., Herrera, S., Fernandez-Alba, A.R., Garcia-Calvo, E., Rosal, R., 2012. Oxidative and photochemical processes for the removal of galaxolide and tonalide from wastewater. Water Res. 46, 4435–4447.

Schiavone, A., Kannan, K., Horii, Y., Focardi, S., Corsolini, S., 2010. Polybrominated diphenyl ethers, polychlorinated naphthalenes and polycyclic musks in human fat from Italy: comparison to polychlorinated biphenyls and organochlorine pesticides. Environ. Pollut. 158, 599–606.

So, S., Wille, U., da Silva, G., 2014. Atmospheric chemistry of enols: a theoretical study of the vinyl alcohol + OH + $O_2$ reaction mechanism. Environ. Sci. Technol. 48, 6694–6701.

Uhle, M.E., Chin, Y.P., Aiken, G.R., McKnight, D.M., 1999. Binding of polychlorinated biphenyls to aquatic humic substances: the role of substrate and sorbate properties on partitioning. Environ. Sci. Technol. 33, 2715–2718.

USEPA (U.S. Environmental Protection Agency), 2016. EPI Suite. https://www.epa.gov/tsca-screening-tools/epi-suitetm-estimation-program-interface#what.

Wang, Z., Chen, J., Sun, Q., Peijnenburg, W.J.G.M., 2011. C60-DOM interactions and effects on C60 apparent solubility: a molecular mechanics and density functional theory study. Environ. Int. 37, 1078–1082.

Wenk, J., von Gunten, U., Canonica, S., 2011. Effect of dissolved organic matter on the transformation of contaminants induced by excited triplet states and the hydroxyl radical. Environ. Sci. Technol. 45, 1334–1340.

Zhao, Y., Truhlar, D.G., 2008a. Density functionals with broad applicability in chemistry. Accounts Chem. Res. 41, 157–167.

Zhao, Y., Truhlar, D.G., 2008b. The M06 suite of density functionals for main group thermochemistry, thermochemical kinetics, noncovalent interactions, excited states, and transition elements: two new functionals and systematic testing of four M06-class functionals and 12 other functionals. Theor. Chem. Acc. 120, 215–241.

Zhao, C.Y., Boriani, E., Chana, A., Roncaglioni, A., Benfenati, E., 2008. A new hybrid system of QSAR models for predicting bioconcentration factors (BCF). Chemosphere 73 (11), 1701–1707.

Zhou, H., Huang, X., Gao, M., Wang, X., Wen, X., 2009. Distribution and elimination of polycyclic musks in three sewage treatment plants of Beijing, China. J. Environ. Sci. 21 (5), 561–567.